Available online www.jsaer.com

Journal of Scientific and Engineering Research, 2018, 5(12):62-68

ISSN: 2394-2630
CODEN(USA): JSERBR

Research Article

Height of F2-layer peak parameter effects on critical frequency by IRI

Emmanuel Nanéma[1]*, Jean Louis Zerbo[2], Moustapha Konaté[3], Frédéric Ouattara[3]

[1]Centre National de la Recherche Scientifique et Technologique (CNRST), Institut de Recherche en Sciences Appliquées et Technologies (IRSAT), 03 BP 7047 Ouagadougou 03, Burkina Faso
[2]Université Nazi BONI (UNB), UFR/ST, 01 BP 1091 Bobo-Dioulasso 01, Burkina Faso
[3]Université Norbert ZONGO (UNZ), Laboratoire de Recherche en Météorologie de l'Espace (LAREME), Koudougou, Burkina Faso

Abstract The purpose of this work is to develop a theoretical approach to find the effects of height of F2-layer peak (hmF2) parameter on critical frequency in F2-layer (foF2). hmF2 and foF2 parameters data are carried out from International Reference Ionosphere model. Height of F2-layer peak (hmF2) and critical frequency in F2-layer (foF2) time values are obtained by running the model under quiet time conditions. This study uses minimum and maximum of solar cycle 22 at Ouagadougou station, in West Africa. Under quiet time conditions and with help of modeling assumptions, the ionosphere parameters are carried out. This study also presents the seasonal effects on height of F2-layer peak and critical frequency profiles. It proposes a new approach to calibrate radio transmitters based on a graphic method. This graphic method matches hmF2 and foF2 profiles by time parameter.

Keywords Ionosphere, height of F2-layer peak, critical frequency in F2-layer, solar cycle phase, IRI model

Introduction

The major constituents of ionosphere layer are N_2, O_2, and O, principally in the thermosphere. Ultraviolet and X-rays coming from the sun cause ionization of chemical components in this layer. Thus, O^+, NO^+, O^{2+} and e^- appear in ionosphere [1]. This layer behaves like plasma and so, is electrically neutral. Because of its constituents in particles, ionosphere is the site of radio waves reflection. F2-layer of ionosphere reflects radio waves because of its density in electrons. This work deals with a theoretical approach to carry out critical frequency values of radio waves corresponding to a given value of height of F2-layer peak in the ionosphere region. Above critical frequency value in F2-layer, radio waves pass through ionosphere layer without being reflected and so, communication is not possible. Many models have been developed to investigate ionosphere layer [2]-[13]. This study uses International Reference Ionosphere (IRI) for ionosphere modeling. IRI is an empirical model which uses data recorded on ionosondes. The model enables to carry out ionosphere parameters. The position of height of F2-layer (hmF2) is linked to the critical frequency (foF2) value. This shows how hmF2 can affect foF2 behavior.

2. Methodology

In this study, modeling assumptions are quiet time conditions for solar cycle phases characterized by Aa index inferior to 20 nT. Minimum and maximum of solar cycle phase 22 are considered. They are determined by the yearly average of Zürich sunspot number Rz. Minimum solar cycle phase is obtained for Rz< 20, while maximum is for Rz> 100. The characteristic month of each season in the year is March for spring, June for summer, September for autumn and December for winter. For each month, the five quietest days are used in the study [14]-[16]. Running IRI model needs to locate the station by its latitude and longitude positions. In this work, Ouagadougou station is used. The site is located in West Africa. The latitude and longitude of this station are respectively 12,4°N and 358,5°E. Local time in Ouagadougou is GMT hour. hmF2 and foF2 profiles are obtained using the hourly variability of these parameters by running IRI model under its 2012 version.

The modeling assumptions enable to get the following equations:

For critical frequency time variation values

$$\mathbf{foF2_i} = \frac{\sum_{j=1}^{n} \mathbf{foF2_{i,j}}}{\mathbf{n}} \quad (1)$$

where $foF2_i$ is the hourly mean value of critical frequency for a selected month at i hour; $foF2_{i,j}$ pointing out the hourly average value of critical frequency at i hour, and j quiet day, n the number of quiet days. In the study, n = 5.

For height of F2-layer time variation values

$$\mathbf{hmF2_i} = \frac{\sum_{j=1}^{n} \mathbf{hmF2_{i,j}}}{\mathbf{n}} \quad (2)$$

where $hmF2_i$ is the hourly mean value of height of F2-layer for a selected month at i hour; $hmF2_{i,j}$ pointing out the hourly average value of height of F2-layer at i hour, and j quiet day, n the number of quiet days. In the study, n = 5.

For each month of solar maximum or minimum, the average values $foF2_{mean}$ and $hmF2_{mean}$ of critical frequency and height of F2-layer peak parameters are given by the following equations:

For $foF2_{mean}$ value

where $foF2_k$ is the critical frequency value at k hour and m the number of values (m = 24).

For $hmF2_{mean}$ value

$$\mathbf{hmF2_{mean}} = \frac{\sum_{k=0}^{m} \mathbf{hmF2}_k}{\mathbf{m}} \quad (4)$$

where $hmF2_k$ is the height of F2-layer peak value at k hour and m the number of terms (m = 24).

3. Results and discussion

Running IRI 2012 under these conditions and with help of the study assumptions, critical frequency and height of F2-layer peak parameters are carried out. Then, mean values of these parameters are calculated and time variation profiles are represented on Figure 1 for minimum solar cycle phase and Figure 2 for maximum solar cycle phase. On Figure 1, panels (a), (b), (c) and (d) represent foF2 and hmF2 time profiles respectively on spring, autumn, summer and winter on minimum solar cycle phase. hmF2 profile is represented on primary Y axis while foF2 is represented on secondary Y axis. X axis determines local time in Ouagadougou. Panels (a) and (b) point out equinox season of hmF2 and foF2 time variations while panels (c) and (d) point out solstice season time variations of the parameters. On Figure 2, panels (a'), (b'), (c') and (d') represents foF2 and hmF2 time profiles respectively on spring, autumn, summer and winter on maximum solar cycle phase. hmF2 profile is represented on primary Y axis while foF2 is represented on secondary Y axis. X axis determines local time in Ouagadougou. Panels (a') and (b') point out equinox season of hmF2 and foF2 time variations while panels (c') and (d') point out solstice season time variations of the parameters.

Panels (a), (b), (c) and (d) of Figures 1 and panels (a'), (b'), (c') and (d') of Figure 2 present foF2 and hmF2 time profiles during solar minimum and maximum of C22 at Ouagadougou station. The primary Y axis represents hmF2 time variation while the secondary Y axis is foF2 time variation. X axis represents local time at Ouagadougou station.

On Figure 1 (panels (a), (b), (c) and (d)), foF2 time profiles highlight "Reversed profile". This result has been previously found [17]. hmF2 time variations present a peak at 12.00 LT. That means that at this time, ionosphere F2-layer raises to its highest level at Ouagadougou station. At the same time, critical frequency of F2-layer doesn't get its highest value. So, during minimum of solar cycle at Ouagadougou station, the peak of hmF2 doesn't correspond to the maximum value of foF2 [18]. Radio waves can easily penetrate ionosphere layer.

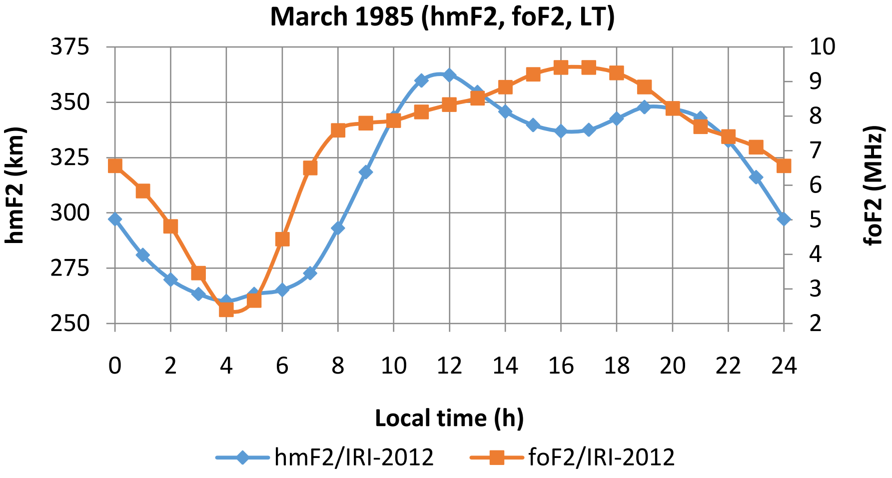

Panel (a): hmF2 and foF2 profiles on March 1985

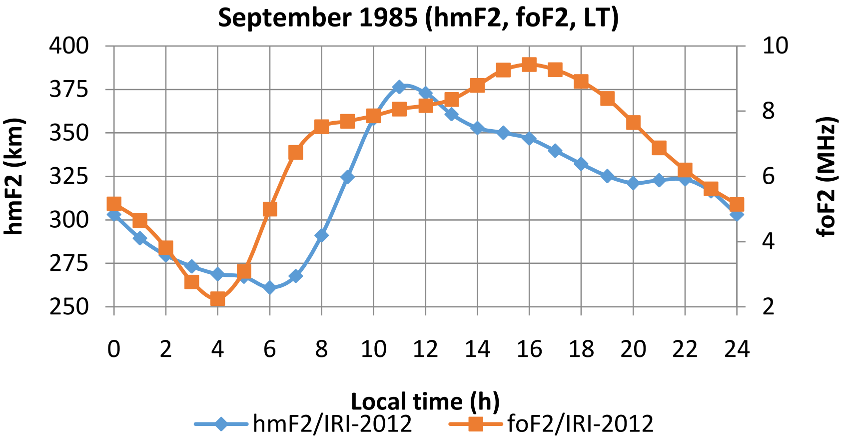

Panel (b): hmF2 and foF2 profiles on September 1985

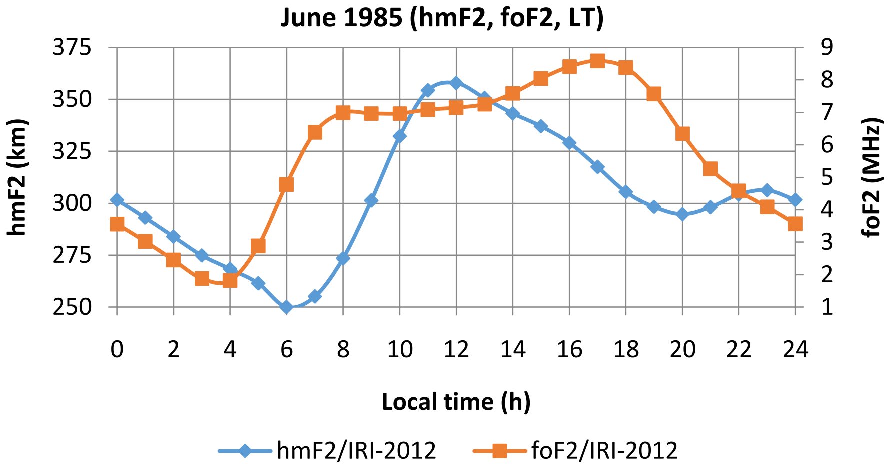

Panel (c): hmF2 and foF2 profiles on June 1985

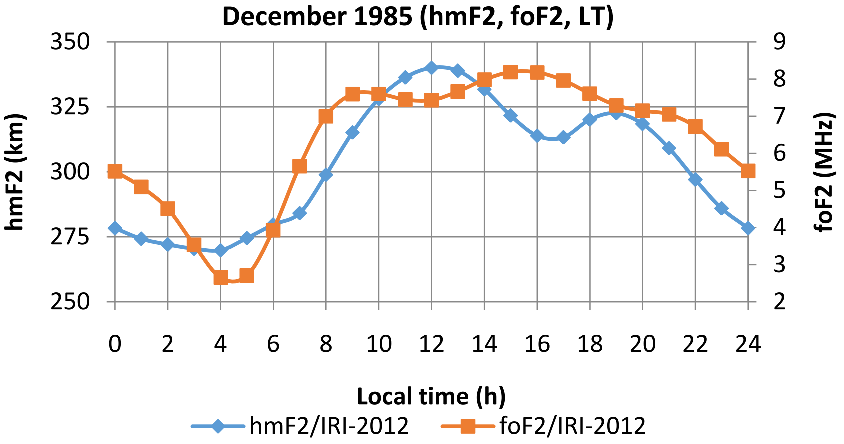

Panel (d): hmF2 and foF2 profiles on December 1985

Figure 1: hmF2 and foF2 profiles during minimum solar cycle phase

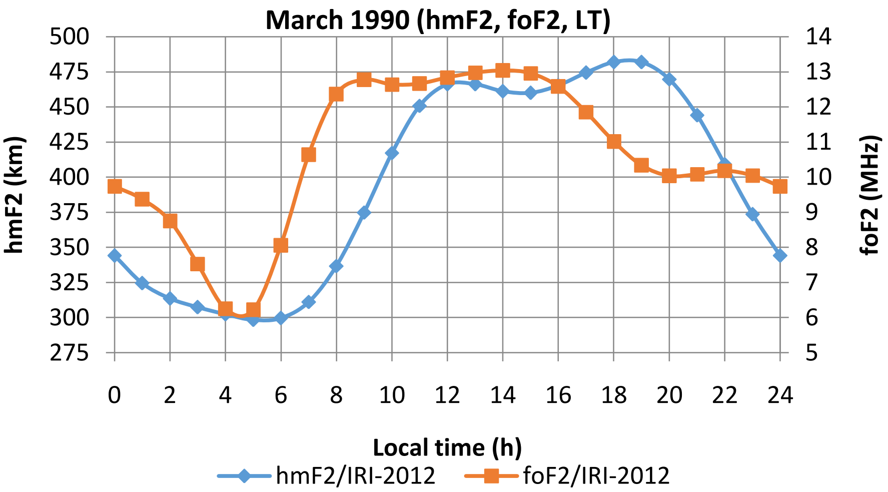

Panel (a'): hmF2 and foF2 profiles on March 1990

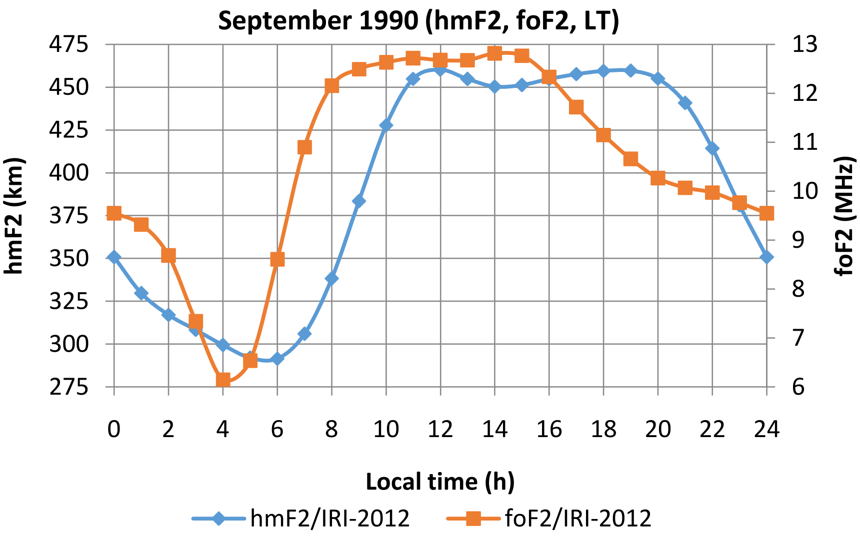

Panel (b'): hmF2 and foF2 profiles on September 1990

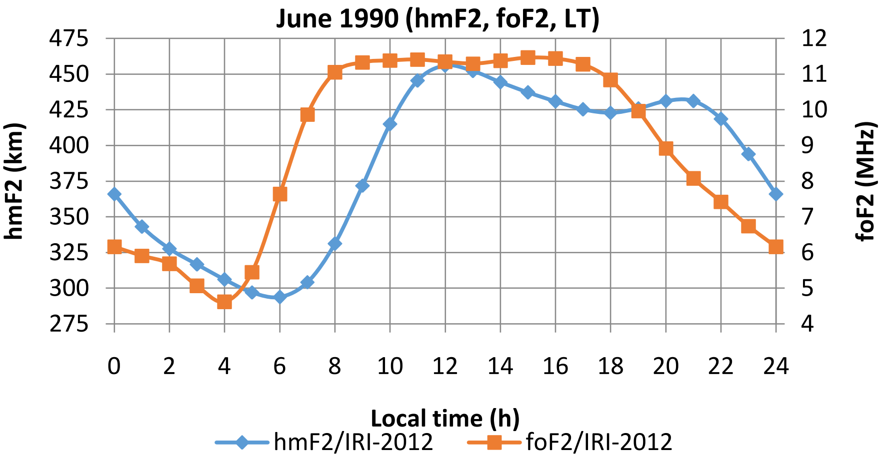

Panel (c'): hmF2 and foF2 profiles on June 1990

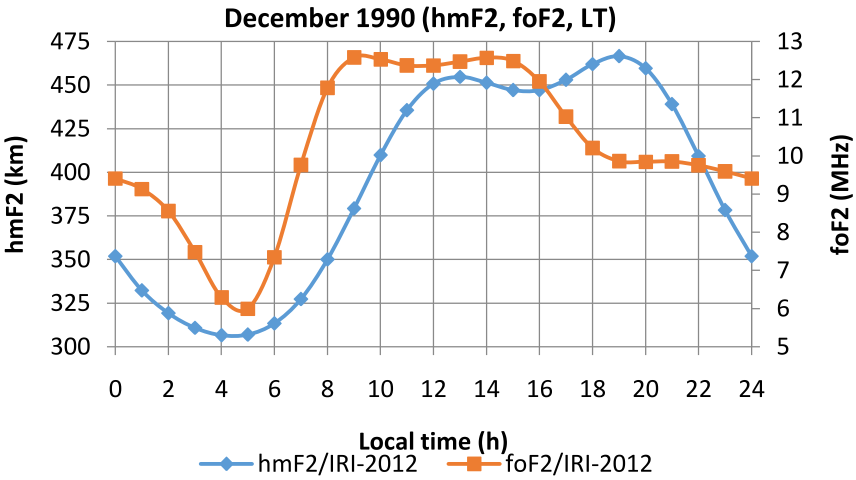

Panel (d'): hmF2 and foF2 profiles on December 1990

Figure 2: hmF2 and foF2 profiles during maximum solar cycle phase

Figure 2 (panels (a'), (b'), (c') and (d')) shows "Plateau profile" on foF2 time variations. hmF2 time variations highlight "Noon bite out" at maximum solar cycle phase.

"Reversed profile" at minimum solar cycle phase and "Plateau profile" at maximum solar cycle on foF2 time variations have previously been found. This study shows that during minimum solar cycle phase, hmF2 time variation presents a peak at 12.00 LT and "Noon bite out" on maximum solar cycle phase.

Using equations (3) and (4), $hmF2_{mean}$ and $foF2_{mean}$values are calculated at minimum and maximum of solar cycle 22.

Table 1: $hmF2_{mean}$ and $foF2_{mean}$ values

	Characteristic months of solar cycle 22							
	Minimum (1985)				**Maximum (1990)**			
	March 85	**June 85**	**Sept. 85**	**Dec. 85**	**March 90**	**June 90**	**Sept. 90**	**Dec. 90**
$hmF2_{mean}/20$ (km)	15.77784	15.186	15.85424	15.1432	19.75596	19.30772	19.57784	19.62612
$foF2_{mean}$ (Mhz)	7.07236	5.660824	6.666032	6.321792	10.58744	8.877976	10.54070	10.18675

Figure 3 highlights the graphic representation of Table 1 values

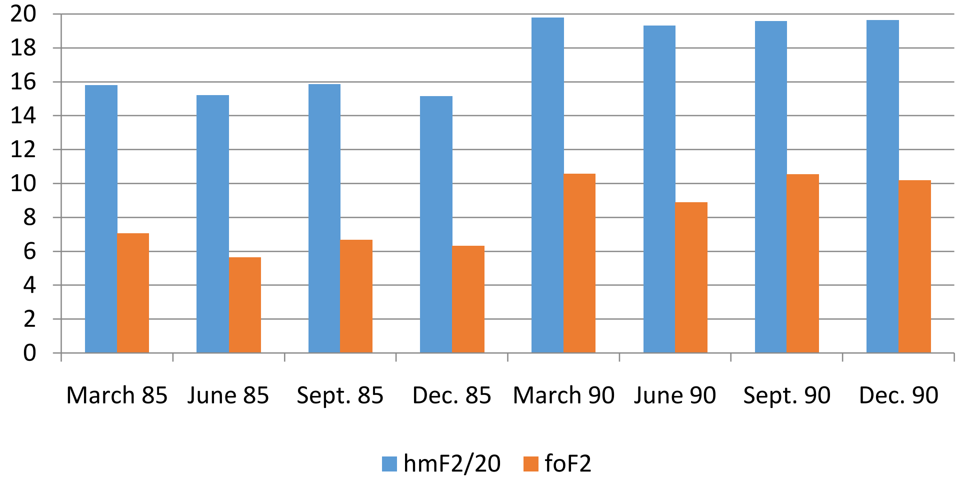

Figure 3: Height of foF2-layer peak and Critical frequency mean values in ionosphere layer

Figure 3 highlights "winter anomaly" on foF2 during minimum and maximum solar cycle phase of C22. This phenomenon is also brought out on hmF2 during maximum solar cycle phase but not during solar minimum.

On any panel, any hmF2 value selected on the time profile can be projected vertically to X axis. The vertical line from this point (hmF2 selected value) to the X axis intersects foF2 profile at a unique point. This intersection point is unique on foF2 time profile. Projecting this intersection point on the secondary Y axis leads to a unique value of foF2. This unique value found on the secondary Y axis is the critical frequency given by hmF2 selected value. So, a given hmF2 value leads to a unique foF2 value. The knowledge of height of F2-layer leads to the critical frequency in the F2-layer. This is a graphic method to determine critical frequency in F2-layer by use of ionosphere position. This graphic method of determining critical frequency in F2-layer by use of ionosphere position enables to calibrate radio transmitters at each level of ionosphere layer. This is a theoretical approach using data from ionosondes in IRI model to calibrate radio transmitters which is different from the usual method based on local time.

4. Conclusion

This work shows height of F2-layer and critical frequency in F2-layer behavior during solar minimum and maximum at Ouagadougou station under quiet time conditions for solar cycle 22 by running International Reference Ionosphere model. "Winter anomaly" is highlighted in this study on hmF2 time profile on solar minimum and maximum. This is a new result found on hmF2 parameter by running IRI. The study also shows ionosphere height of F2-layer effects on critical frequency. hmF2 and foF2 time profiles carried out in this study lead to a theoretical approach to calibrate radio transmitters for telecommunication by help of a graphic method. This approach requires the knowledge of foF2 and hmF2 parameters for a given month. Time is used to match foF2 and hmF2 parameters but is not used to carry out foF2 value for a given hmF2.

References

[1]. Rishbeth, H. and Garriott O. K. (1969) *Introduction to ionospheric physics*, International Geophysics Series, Academic Press, New York and London, Edited by J. Van Mieghem, pp.120-121.

[2]. Pedatella, N. M., Forbes, J. M., Maute, A., Richmond, A. D., Fang, T.-W., Larson, K. M., and Millward, G. (2011) Longitudinal variations in the F region ionosphere and the topside ionosphere-plasmasphere: Observations and model simulations, *Journal of Geophysical Research*, 116, A12309, doi:10.1029/2011JA016600.

[3]. Roble, R. G., Ridley, E. C., Richmond, A. D., Dickinson, R. E. (1988) A coupled thermosphere/ionosphere general circulation model, *Geophysics Research Letter*, 15, 1325

[4]. Wang, W., Wiltberger, M., Burns, A.G., Solomon, S.C., Killeen, T.L., Maruyama, N., and Lyon, J.G. (2004) Initial Results from the Coupled Magnetosphere-Ionosphere-Thermosphere Model: Thermosphere-Ionosphere Responses, *Journal of Atmospheric and Solar-Terrestrial Physics*, 66/15-16, 1425.

[5]. Richmond, A. D., E. C. Ridley, and R. G. Roble (1992) A thermosphere/ionosphere general circulation model with coupled electrodynamics, *Geophysics Research Letter*, 19, 601

[6]. Burns, A. G., Wang, W., Killen, T. L., and Solomon, S. C. (2004) A "tongue" of neutral composition, *Journal of Atmospheric and Solar-Terrestrial Physics*, 66, 1457-1468, doi:10.1016/j.jastp.2004.04.009

[7]. Goodrich, C.C., Sussman, A. L., Lyon, J. G., Shay, M. A., Cassak, P. A. (2004) The CISM code coupling strategy, *Journal of Atmospheric and Solar-Terrestrial Physics*, 66, 1469-1479, doi:10.1016/j.jastp.2004.04.010

[8]. Weimer, D. R. (2005), Improved ionospheric electrodynamic models and application to calculating Joule heating rates, *Journal of Geophysical Research*, 110, A05306, doi: 10.1029/2004JA010884

[9]. Richmond, A.D., Matsushita, S., and Tarpley, J.D., (1976) On the production mechanism of electric currents and fields in the ionosphere. *Journal of Geophysical Research*, 81, 547-555.

[10]. Jin, S. and Park, J.U. (2007) Ionospheric Tomography: A Comparison with the IRI-2001 Model over South Korea. *Earth Planet Space*, 59, 287-292. https://doi.org/10.1186/BF03353106

[11]. Bittencourt, J.A. and Chryssafidis, M. (1994) On the IRI Model Predictions for the Low-Latitude Ionosphere. *Journal of Atmospheric and Solar-Terrestrial Physics*, **56**, 995-1009. https://doi.org/10.1016/0021-9169(94)90159-7

[12]. Ouattara, F. and Rolland, F. (2011) Variability of CODG TEC and IRI 2001 Total Electron Content (TEC) during IHY Campaign Period (21 March to 16 April 2008) at Niamey under Different Geomagnetic Activity Conditions. *Scientific Research and Essays*, **6**, 3609-3622. https://doi.org/10.5897/SRE10.1050

[13]. Qian, L., Burns, A. G., Chamberlin, P. C. and Solomon, S. C. (2010), Flare location on the solar disk: Modeling the thermosphere and ionosphere response, *Journal of Geophysical Research*, 115, A09311, doi:10.1029/2009JA015225

[14]. Ouattara, F., Nanéma, E. (2014) Quiet time foF2 variation at Ouagadougou station and comparison with TIEGCM and IRI-2012 predictions for 1985 and 1990, *Physical Science International Journal*, 4 (6), 892-902.

[15]. Ouattara, F. (2013) IRI-2007 foF2 Predictions at Ouagadougou Station during Quiet Time Periods from 1985 to 1995. Archives of Physics Research, 4, 12-18.

[16]. Ouattara, F. and Nanéma E. (2013) hmF2 quiet time variations at Ouagadougou and comparison with IRI-2012 and TIEGCM predictions during solar minimum and maximum, *Archives of Applied Science Research*, 5(5):55-61.

[17]. Nanéma, E., Ouédraogo, I., Zoundi, C., and Ouattara, F. (2018) Electron bulk Surface Density Effect on Critical Frequency in the F2-Layer. *International Journal of Geosciences*, **9**, 572-578. https://doi.org/10.4236/ijg.2018.99033

[18]. Nanéma, E., Gnabahou, D. A., Zoundi, C., and Ouattara, F. (2018) Modeling the Ionosphere during Quiet Time Variation at Ouagadougou in West Africa. *International Journal of Astronomy and Astrophysics*, **8**, 163-170. https://doi.org/10.4236/ijaa.2018.820311.